Clinical and Experimental Obstetrics & Gynecology

Clin. Exp. Obstet. Gynecol. **2025**; 52(1): 25783
https://doi.org/10.31083/CEOG25783

Original Research

Concordance of Prenatal Ultrasonography and Magnetic Resonance Imaging in the Classification of Corpus Callosum Dysplasia

Hui Peng[1,†], Xi Chen[2,†], Xuejin Zou[3], Yan Song[3], Chunlan Cheng[4], Jianli Zhang[1,*]

[1]Department of Imaging, Wenjiang District Maternal and Child Health Hospital, 611100 Chengdu, Sichuan, China
[2]Department of Ultrasound, Sichuan Provincial Maternity and Child Health Care Hospital, 610045 Chengdu, Sichuan, China
[3]Department of Radiology, Sichuan Provincial Maternity and Child Health Care Hospital, 610045 Chengdu, Sichuan, China
[4]Department of Clinical Laboratory, Sichuan Provincial Maternity and Child Health Care Hospital, 610045 Chengdu, Sichuan, China
*Correspondence: 358992904@qq.com (Jianli Zhang)
[†]These authors contributed equally.
Academic Editor: Michael H. Dahan
Submitted: 21 July 2024 Revised: 4 November 2024 Accepted: 9 December 2024 Published: 14 January 2025

Abstract

Background: Prenatal ultrasound has always been difficult to classify fetal corpus callosum abnormalities. This paper aims to evaluate the added value of fetal magnetic resonance imaging (MRI) to ultrasound in detecting fetal corpus callosum anomalies and the consistency of the classification of prenatal ultrasound and magnetic resonance imaging for corpus callosum anomalies. **Methods**: A retrospective analysis was performed of fetuses with abnormal cavum septi pellucidi who had ultrasonography and MRI in utero in Sichuan Maternal and Child Health Hospital and Wenjiang District Maternal in China and Child Health Hospital from January 2018 to December 2023. Fetal corpus callosum anomalies are classified according to the severity of the findings. The classification results of MRI were used as the diagnostic criteria. The findings detected on ultrasound (US) were compared to those detected on MRI. and the receiver operating characteristic (ROC) curve was used to analyze the sensitivity and specificity of prenatal ultrasound in diagnosing corpus callosum anomalies. The Kappa test was used to analyze the consistency of prenatal ultrasound and MRI in the classification of corpus callosum anomalies. **Results**: Of the 203 cases of fetuses with abnormal cavum septi pellucidi, 143 cases (70.4%) were normal, 34 cases (16.7%) had complete agenesis of the corpus callosum, and 18 cases (8.9%) had partial agenesis of the corpus callosum. Eight cases (3.9%) had dysplasia of the corpus callosum. The area under the ROC curve of prenatal ultrasound for the diagnosis of corpus callosum anomalies was 0.840 (95% confidence interval (CI) 0.782–0.888), the sensitivity was 75.00%, and the specificity was 93.01%, The positive likelihood ratio was 10.7 and the negative likelihood ratio was 0.3. Prenatal ultrasonography and MRI had moderate concordance in the classification of corpus callosum anomalies (Kappa = 0.673, $p < 0.001$). The concordance was good in diagnosing complete agenesis of the corpus callosum (Kappa = 0.862, $p < 0.001$), while the concordance was moderate in diagnosing partial agenesis of the corpus callosum (Kappa = 0.643, $p < 0.001$). **Conclusions**: Prenatal ultrasonography is accurate and effective in the diagnosis of corpus callosum anomalies. Magnetic resonance imaging can provide more information in the classification of corpus callosum anomalies and the diagnosis of neurologic complications. The MRI should be combined with ultrasonographic transverse, midsagittal, and coronal views to evaluate the classification of corpus callosum anomalies.

Keywords: prenatal ultrasound; magnetic resonance imaging; corpus callosum agenesis; Kappa

1. Introduction

Abnormality of the corpus callosum is divided into three types: complete absence of corpus callosum (complete agenesis of the corpus callosum (CACC)), partial loss of the corpus callosum (partial agenesis of the corpus callosum (PACC)), and hypoplasia of corpus callosum (HpCC) which is a thin or small corpus callosum [1]. The cavum septi pellucidi is closely related to the embryonic origin of the corpus callosum, and the abnormal development of the cavum septi pellucidi suggests the abnormal development of the corpus callosum and other structures [2,3]. Magnetic resonance is of great value for the evaluation of normal fetal anatomy [4] and the diagnosis of birth defects, especially the prenatal diagnosis of the central nervous system abnormalities [5,6]. According to literature reports, different types of simple corpus callosum developmental abnormalities have a different prognosis. Both CACC and PACC have a high risk of chromosomal abnormalities [1,7]. Abnormalities of the corpus callosum are strongly associated with early-onset epilepsy with Aicardi syndrome. The incidence of different types of corpus callosum abnormalities in this disease varies [8]. Accurate classification of corpus callosum abnormalities is particularly important. The use of fetal magnetic resonance imaging (MRI) is valuable in the classification of abnormalities of the corpus callosum after the confirmation of a suspected diagnosis on prenatal ultrasound [9]. Previous article had mainly focused on prenatal ultrasound and magnetic resonance diagnosis of the corpus callosum [10]. However, few articles have reported the consistency of the two methods in classification of corpus callosum abnormalities [11]. This study aims to eval-

uate the efficacy of prenatal ultrasound in the diagnosis of corpus callosum abnormalities and analyze the consistency of ultrasound and magnetic resonance examinations on the classification of corpus callosum abnormalities.

2. Materials and Methods

2.1 Patient Data

The singleton fetus imaged in Wenjiang District Maternal in China and Child Health Hospital and Sichuan Maternal and Child Health Hospital in China from January 2018 to December 2023 was selected as the study image, with inclusion criteria being: (1) Abnormal cavum septi pellucidi in prenatal ultrasound screening; (2) Those who have completed the fetal cranial MRI examination within about a week of prenatal ultrasound; (3) A written consent was signed by the patients or their families/legal guardians. And the exclusion criteria were: (1) Patients whose fetal cranial MRI images cannot be clearly classified; (2) Those cases were lost to be followed by clinical care or telephone contact.

2.2 Methods

Ultrasound examination was performed utilizing either General Electric Company volusion E8 (GE Healthcare, Zipf, Austria), Mindray Resona 8S (Mindray Resona, Shenzhen, Guangdong, China) color Doppler ultrasound diagnostic instrument, transabdominal probe (probe frequency 2–5 MHz) and transvaginal 3 dimensional volume probe (probe frequency 5–9 MHz). Pregnant patients were taken in the supine position and scanned through the abdomen. Prenatal examination was conducted according to the Guidelines for Ultrasound Examination (2012) of Ultrasound Branch of Chinese Medical Doctor Association [12], and the transverse view of the fetal brain was retained. When the abnormal development of the fetal corpus callosum was suspected by the abnormal morphology of the transparent septum cavity, the fetal sagittal views were obtained by two-dimensional and three-dimensional ultrasound. Focus was placed on the following contents: 1. Direct signs: observe the morphology, size and integrity of the corpus callosum on the median sagittal view. In the median sagittal view of the fetal brain, the corpus callosum is located below the cingulate gyrus and above the thalamus, and is strip-like hypoechoic; 2. Indirect signs: (1) Cavum septi pellucidi (CSP) abnormal morphology: a. The width of cavum septi pellucidi beyond the 95th percentile values of CSP (3.7–7 mm) [13]; b. Ratio of anterior-to-posterior diameter to transverse diameter (L/W) is less than 1.5 [14]; c. Absence of CSP; (2) Lateral ventricle expansion: The value of the lateral ventricle body is greater than 1 mm; (3) "Teardrop change": The lateral ventricles lose their normal morphology, with the anterior horns and anterior parts of the body slender and the posterior parts of the body rounded and blunt, resembling teardrops; (4) Three echogenic lines running parallel in the upper cranium, the middle one representing the falx cerebri, the lateral ones representing the medial borders of the separated hemispheres, the "three lines sign"; (5) Midline thalamic posterior cystic mass; (6) Pericallosal artery disappearing or abnormal morphology with color Doppler not collecting signals from the pericallosal artery above the corpus callosum or color Doppler only collecting part of the pericallosal artery signal above the corpus callosum, and the pericallosal artery is abnormal; (7) Combined with intracranial and external anomalies. Finally, two physicians qualified for prenatal diagnosis made a clear diagnosis together, and the MRI examination results were not known at the time of diagnosis. All subjects gave their informed consent for inclusion before they participated in the study. The study was conducted in accordance with the Declaration of Helsinki, and the protocol was approved by the Ethics Committee of Wenjiang District Maternal and Child Health Hospital (approval number: WJFY2022LSLY-032).

All fetal MRI examinations were performed via a GE Signa HDx 1.5T (GE Medical Systems, Waukesha, WI, USA) with an 8-channel abdominal phased array coil. The patient was lying on the examination table, supine or lateral, with her head going first. The mother was scanned in three planes to determine the fetal position. The fetal head was then scanned in three directions: coronal, sagittal, and axial, with the last image serving as the baseline for each scan to assure image positioning accuracy. The scanning sequences used and parameters were as follows: (1) T2-weighted of single-shot fast spin echo (SS FSE) with coronal, sagittal, and axial directions, slice thickness 4 mm, gap 0.5 mm, field of view (FOV) 380 mm $\times$ 380 mm, echo time (TE) 100 ms, repetition time (TR) 1800 ms, and matrix 320 $\times$ 256. (2) Axial three dimensional (3D) fast imaging employing steady state acquisition (3D FIESTA), slice thickness 3 mm, FOV 380 mm $\times$ 380 mm, TE minimum, TR minimum, flip angle 65°, and matrix of 320 $\times$ 256. (3) Axial T1-weighted of fast spoiled gradient echo (FSPGR), slice thickness 4 mm, gap 0.5 mm, FOV 380 mm $\times$ 380 mm, TE min full, TR 155 ms, flip angle 80°, and matrix of 228 $\times$ 160. (4) Axial diffusion-weighted imaging (DWI), b value 600, slice thickness 4 mm, gap 0.5 mm, FOV 380 mm $\times$ 380 mm, TE minimum, TR 4200 ms, and matrix 128 $\times$ 130. The scanning time was about 12–17 minutes. Two radiologists separately examined the fetal brain's shape, size, and signal, as well as the anatomy of the corpus callosum and other abnormalities, with ultrasound data unknown at the time of diagnosis.

Classification criteria of the corpus callosum was the same in both ultrasound (US) and MRI: (1) Normal, normal sagittal length and complete parts of the mouth, knee, body, and pressure, with normal thickness; (2) CACC, refers to corpus callosum not displayed; (3) PACC, refers to only display part of the corpus callosum, including part of the mouth, genu, body and splenium; and (4) HpCC, refers to the short or thin corpus callosum. Malinger G *et al.* [15]

Table 1. Basic information and prenatal ultrasound image characteristics of the 203 cases.

Types (NO.)	Gravida age (year) #	Ultrasound gestational weeks (week) #	Direct sign (%)		Indirect sign (%)								
			Middle sagittal view in 2D*	Sagittal tangent view in 3D*	Abnormal CSP			Lateral ventricle dilates*	"Tear sign" *	"Three-lines sign" *	Cystic behind thalamic*	Upper third ventricle*	Abnormal pericallosal artery*
					Missing*	L/W <1.5*	Narrow*						
CACC 34	28.1 (26.4, 29.8)	26.8 (25.0, 28.7)	19 (55.9)	5 (14.7)	32 (94.1)	1 (2.9)	1 (2.9)	28 (82.3)	18 (52.9)	22 (64.7)	16 (47.1)	6 (17.6)	15 (44.1)
PACC 18	28.3 (26.3, 30.4)	27.3 (25.4, 29.1)	11 (61.1)	2 (25.0)	-	2 (11.1)	2 (11.1)	17 (94.4)	2 (11.1)	3 (16.7)	8 (44.4)	1 (5.5)	4 (22.2)
HpCC 8	30.6 (25.9, 35.4)	28.7 (25.4, 32.1)	5 (62.5)	4 (50.0)	-	1 (12.5)	-	2 (2.5)	-	-	2 (2.5)	-	-
Normal 143	27.9 (27.3, 28.7)	26.8 (26.2, 27.4)	60 (41.9)	53 (37.0)	-	2 (1.4)	101 (92.0)	8 (5.6)	-	-	2 (1.4)	-	-

Note: NO., number; Non-normally distributed continuous variables are shown as median (interquartile range). #, data are medians, data in parentheses are the interquartile range; categorical variables are shown as n [%]. *, data are medians, data in parentheses are the interquartile range; CACC, complete corpus callossum loss; PACC, partial corpus callossum loss; HpCC, corpus callosum dysplasia; Normal, normal corpus callosum; CSP, cavum septi pellucidi; L/W, ratio of anterior-to-posterior diameter to transverse diameter; 2D, two-dimensional; 3D, three-dimensional.

data was used as the reference standard for the thickness and length of the corpus callosum.

2.3 Statistical Analysis

Statistical analysis was performed using SPSS 24.0 software (IBM, Armonk, NY, USA) and MedCalc software version 11.4.2.0 (MedCalc Software, Mariakerke, Belgium). Measurement data were expressed by mean and standard deviation (SD) or median (P25, P75) based on the data distribution format in the manuscript, the number and percentage were used for non-missing values of categorical variables. The difference between the two continuous variables was assessed by *T*-test and non-parametric test as appropriate. Using MRI results, the sensitivity, the specificity, the positive likelihood ratio, and the negative likelihood ratio of ultrasound were calculated for the diagnosis of abnormal corpus callosum development. The diagnostic efficacy of prenatal ultrasound on the abnormality of the corpus callosum was analyzed using receiver operating characteristic curve (ROC). The Kappa method was used to evaluate the level of agreement between the two diagnostic modalities and between the two observers per each modality. Kappa Consistency classification: poor consistency (Kappa = 0.00–0.20), general consistency (Kappa: 0.21–0.40), moderate consistency (Kappa: 0.41–0.60), good consistency (Kappa: 0.61–0.80), and excellent consistency (Kappa: 0.81–1.00). Two-sided $p < 0.05$ was considered as a statistically significant difference.

3. Results

3.1 Basic Information

Two hundred and three patients were studied and the mean age was 28.2 (18, 40) years old. The gestational age was 26.9 (20.6, 36.1) weeks on US, and the gestational age was 27.1 (20.7, 36.4) weeks on MRI. There was no significant difference in gestational age between ultrasound and MRI examinations (Z = –10.183, $p < 0.001$). Among the 203 included fetuses, 29 had arachnoid cysts (14.3%) in brain midline, 1 had intracranial hemorrhage (0.5%), 1 had cerebellar vermis dysplasia (0.5%), 5 had cerebral cortical malformation (2.5%) and 1 had midline lipoma (0.5%). Among these, 2 cases midline cyst, 1 arachnoid cyst in the posterior fossa, and 1 cerebral cortical malformation had missed on ultrasound (Fig. 1). Of the 203 cases, 15 decided to terminate the pregnancy (7.4%), one case of fetus with normal corpus callosum development showed strabismus after birth. Genetic testing of an HpCC patient confirmed a 10.36 Mb heterozygous deletion in the *6q25.3q27* region, which was a pathogenic copy number variation. and 8 cases were lost to follow-up (3.9%). The infant health care results of the remaining fetuses showed no abnormality after birth.

Prenatal ultrasound images were analyzed for the included cases. Direct signs: In 203 cases, 95 cases (46.8%) had obtained sagittal views successfully by 2D scanning, and 64 cases (31.5%) showed median sagittal views by 3D scanning. Indirect signs: in CACC, 34 cases had abnormal cavum septi pellucidi (100%). The occurrence rate of other indirect signs ranged from high to low as lateral ventricle expansion, presence of "three lines sign", the "teardrop" sign of the lateral ventricle, cystica behind thalamic widening, abnormal pericallosal artery, and lifting of the third ventricle. In cases of PACC, 2 (11.1%) had the length/width of the cavum septi pellucidi being less than 1.5, and 2 (11.1%) had small cavum septi pellucidi (Table 1).

3.2 Analysis of the Diagnostic Efficacy of Prenatal Ultrasound for Corpus Callosum Abnormalities

Of the 203 fetuses, 60 (29.6%) were diagnosed as abnormal corpus callosum, and 143 (70.4%) as normal by MRI. Utilizing ultrasound, the results were 56 (27.6%) and 147 (72.4%). Prenatal ultrasound diagnosis of abnormal corpus callosum had the area under the curve being 0.840 (95% CI 0.782–0.888) (Table 2, Fig. 2).

3.3 Consistent Analysis of Classification of Abnormal Corpus Callosum by Prenatal Ultrasound and Magnetic Resonance and Sonogram Characteristics

Of the 203 fetuses, 56 (27.6%) had abnormal corpus callosum according to prenatal ultrasound, in which 36 (64.3%) cases were CACC, 17 (30.3%) cases were PACC, and 3 (5.4%) were HpCC (Table 1).

Sixty (29.6%) had an abnormal corpus callosum according to MRI, in which 34 (56.7%) cases were CACC, 18 (30.0%), cases were PACC and 8 (13.3%) was HpCC (Table 1). Among patients with PACC, there were 2 (11.1%) cases of rostrum dysplasia, 2 (11.1%) cases of body and splenium dysplasia, and 14 (77.8%) cases of splenium dysplasia. Among patients with HpCC, seven cases (87.5%) had short corpus callosum and 1 (12.5%) case had thin corpus callosum.

Table 2. Results of prenatal ultrasound and MRI typing for 203 cases of suspected abnormal corpus callosum development.

Ultrasound	Magnetic resonance				Amount to
	Normal	HpCC	PACC	CACC	
Normal	133	6	7	1	147
HpCC	1	1	1	0	3
PACC	6	1	8	2	17
CACC	3	0	2	31	36
Amount to	143	8	18	34	203

Note: CACC, complete corpus callossum loss; PACC, partial corpus callossum loss; HpCC, corpus callosum dysplasia; Normal, normal corpus callosum; MRI, magnetic resonance imaging.

Prenatal ultrasound and MRI findings showed moderate consistency (Kappa = 0.673, $p < 0.001$) in total. As to CACC, high consistency was noted (Kappa = 0.862, $p < 0.001$) and PACC demonstrated moderate consistency

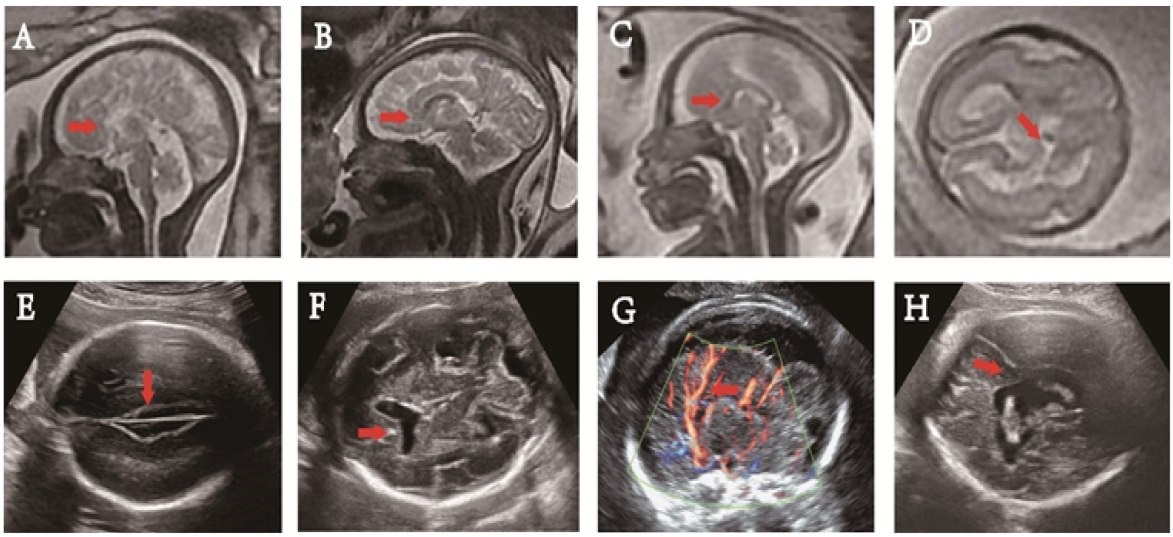

Fig. 1. Prenatal magnetic resonance imaging (MRI) and ultrasound images. (A) The corpus callosum and the cingulate gyrus were not clearly shown at 33+6 weeks in the mid-sagittal view on T2WI, and the cerebral sulci on the medial side of the cerebral hemisphere were arranged radially (red arrow). (B) The absence of rostrum, splenium (red arrow) and the posterior part of the body of the corpus callosum was shown in the mid-sagittal view on T2WI at 35 weeks of gestation. (C) Noted was short corpus callosum (red arrow), and its anteroposterior diameter being about 18 mm at 25+2 weeks in the mid-sagittal view on T2WI. (D) The lateral ventricle wall was interrupted and lateral ventricle communicated with the subarachnoid space (red arrow) at 24+2 weeks of gestation in axial view on T2WI. (E) At 22+2weeks of gestation, the interhemispheric cistern of the brain was enlarged, showing a "three-line sign" (red arrow) in the craniocerebral axial view. (F) At 24+1weeks of gestation, in the cross view of the fetal brain, the septum pellucidum disappeared and anterior horns of the bilateral ventricles communicated (red arrow). (G) There was no clear corpus callosum in the midsagittal view of the fetal brain at 34+5 weeks of gestation with the pericallosal artery running upward at the parietal lobe abnormally (red arrow). (H) A fetus with lobulated holoprosencephaly shown at 31+3 weeks of gestation. The midline of the brain was broken, the brain parenchyma crossed the midline, and the bodies of the bilateral lateral ventricles were connected in axial view (red arrow).

(Kappa = 0.643, $p < 0.001$). Prenatal ultrasound diagnosis of CACC had the area under the curve being 0.941 (95% CI 0.899–0.969), Prenatal ultrasound diagnosis of PACC had the area under the curve being 0.725 (95% CI 0.658–0.786), Prenatal ultrasound diagnosis of abnormal corpus callosum had the area under the curve being 0.560 (95% CI 0.488–0.630) (Table 2, 3).

4. Discussion

The consistency of US and MRI in classification of corpus callosum abnormalities remains unclear. Our study evaluated the Kappa of two methods in classification of corpus callosum abnormalities. One major finding of this study was that prenatal ultrasound and MRI findings showed moderate consistency (Kappa = 0.673). As to CACC, high consistency was noted (Kappa = 0.862) and PACC demonstrated low consistency (Kappa = 0.643). Moreover, the abnormal cavum septi pellucidi was the most common indirect sign in CACC. The occurrence rate of other indirect signs sorted from high to low including lateral ventricle expansion, presence of "three lines sign", the "teardrop" sign of the lateral ventricle, cystica behind thalamic widening, abnormal pericallosal artery, and lifting of the third ventricle.

The incidence of abnormal corpus callosum development in normal live births is about 0.3–0.7% [16], with and incidence of up to 2–3% in children with neurodevelopmental disorders [17]. Prenatal counseling for abnormal development of the corpus callosum is extremely challenging. The abnormal prognosis of the complex corpus callosum is poor, which mainly depends on the type of combined malformations, especially with severe neurologic malformations [18,19]. Different types of simple corpus callosum development abnormalities also have different prognoses [7,20]. Therefore, the prenatal typing of abnormal corpus callosum is particularly important. In this study, prenatal ultrasound can effectively diagnose the abnormal corpus callosum, with high sensitivity, specificity and the area under the curve. Prenatal ultrasound is accurate and effective in diagnosing the abnormal corpus callosum. This study concluded that there was a high consistency and moderate consistency in classification of CACC and PACC. This is similar to previous results by Manevich-Mazor *et al.* [11]. They found a high agreement between ultrasound and MRI in CACC (Kappa: 0.742) and moderate agreement in PACC (Kappa: 0.258). The main reasons for the difficulty in typing partial corpus callosum are as follows: (1) The PACC is not a typical sign as compared with CACC. It has been re-

Table 3. Agreement analysis of classification of abnormal corpus callosum by prenatal ultrasound and MRI examination and AUC of ROC curve of prenatal ultrasound for abnormal corpus callosum development.

	Kappa	*p*	AUC	95% CI	Sensitivity	Specificity	+LR	–LR	*p*
CACC	0.862	<0.001	0.941	0.899 to 0.969	91.18	96.99	30.27	0.09	<0.001
PACC	0.643	<0.001	0.725	0.658 to 0.786	50.00	95.05	10.11	0.53	0.0002
HpCC	0.168	0.001	0.560	0.488 to 0.630	12.50	99.48	24.00	0.88	0.338
Total	0.673	<0.001	0.840	0.782 to 0.888	75.00	93.01	10.73	0.27	<0.001

Note: CACC, complete callosal loss; PACC, partial callosal deletion; HpCC, corpus callosum dysplasia; AUC, the area under the curve; ROC, receiver operating characteristic; +LR, the positive likelihood ratio; –LR, the negative likelihood ratio; CI, confidence interval.

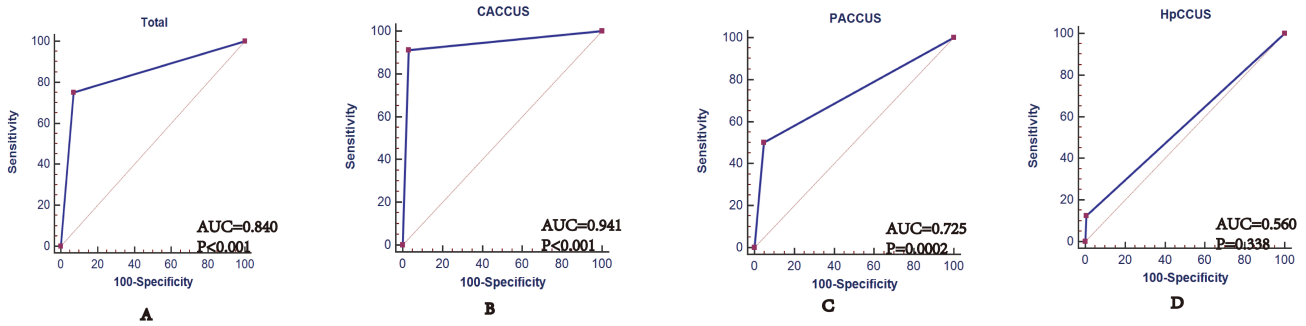

Fig. 2. ROC curve of prenatal ultrasound for abnormal corpus callosum development. (A) ROC curve of prenatal ultrasound for abnormal corpus callosum development. (B) ROC curve of prenatal ultrasound for CACC. (C) ROC curve of prenatal ultrasound for PACC. (D) ROC curve of prenatal ultrasound for HpCC. CACCUS, prenatal ultrasound for complete callosal loss; PACCUS, prenatal ultrasound for partial callosal deletion; HpCCUS, prenatal ultrasound for corpus callosum dysplasia.

ported that the ratio of cavum septi pellucidi (length/width less than 1.5) is an important indicator of partial corpus callosum loss [14]. In this study, 11.1% of patients demonstrated the cavum septi pellucidi ratio, and 11.1% of patients demonstrated a narrow cavum septi pellucidi. (2) As there were partial corpus callosum structures, other indirect signs are not as typical as CACC. (3) When cases had hydrocephalus, lipoma, or intracranial hemorrhage. the mouth and splenium of the corpus callosum in median sagittal views were difficult to identify. The typing accuracy of ultrasound needs to be improved, especially for partial corpus callosum deletion. The choice of imaging view and imaging method is the main determinant of the display of the fetal corpus callosum.

Fetal brain imaging is mainly composed of orthogonal, transverse, sagittal and coronal views. (1) The transverse view of the fetus brain was the most accessible one, which can only assess indirect signs of corpus callosum abnormality. On the transverse view, cavum septi pellucidi abnormality is the most common indirect sign [14,21]. In this study, the incidence of absence of the cavum septi pellucidi of CACC reached 94.1%, but not all corpus callosum abnormalities had related indirect signs in the transverse view. A large proportion of prenatal detected PACC cases had an abnormal CSP shape. This should be considered as another indirect sign of PACC, and is usually the only clue to the diagnosis. When observing this sign in a screening setting, the PACC should be considered and foster an attempt to observe the corpus callossum directly in the median sagittal direction [22]. In this study, the low occurrence rate of indirect signs of PACC was the abnormal cavum septi pellucidi (cavum septi pellucidi ratio was 11.1% and narrow was 11.1%). Zeng *et al.* [2] proposed a method for observing the corpus callosum in three new transverse views to provide more information about the corpus callosum structure. (2) The observation of the callosal structure in the median sagittal view is a direct sign for the diagnosis of corpus callosal abnormalities [23]. However, the display rate of median sagittal views obtained by abdominal 2D ultrasound was low, and the literature reported that the display rates of median sagittal views ranged from 52% to 84% [24]. In this study, the display rate of median sagittal view was approximately 66.7%. Overall, the display rate of the median sagittal view during pregnancy was higher than that of late pregnancy. When the fetal head enters the pelvis, transabdominal ultrasound is often difficult to obtain the median sagittal view of the brain, with the examination being difficult and time-consuming. (3) Coronary view imaging of the brain in the fetus is highly dependent on fetal position as well as physician experience and technology. The International Association for Obstetrics and Gynecology Ultrasound (ISUOG) 2021 guidelines for the ultrasound examination of the fetal central nervous system (Part II) states that “the special examination of fetal

brain anatomy is based on a series of serial scans of sagittal and coronal views based on three transverse views of the fetal brain" [25]. The American Association for Maternity Ultrasound also noted that indirect signs are often detected in the conventional axial scanning view of the fetal brain. Not all signs must occur simultaneously to suspect this diagnosis and prompt detailed neuroimaging is suggested. If possible, an ultrasound should be performed by transvaginally in order to obtain the median and coronal views [26]. This study was retrospective, and only the transverse and lost views of the fetal brain were collected, and no coronal views were analyzed. Further studies can explore the transverse view, along with the median sagittal view combined with the coronal view facing the corpus callosum abnormalities for classification.

The main imaging modalities of abnormal corpus callosum development are two-dimensional ultrasound, three-dimensional ultrasound and magnetic resonance imaging. 2D ultrasound has high resolution and simple operation. However, the two-dimensional craniocerebral transverse views are easy to obtain, but the median sagittal views and coronal views are more difficult to obtain. Three-dimensional ultrasound can obtain the volume data from the transverse view of the fetal head to form three mutually vertical views. The C view is the median sagittal view of the brain. However, the image quality obtained by 3D reconstruction is far less than 2D images, and the diagnosis of corpus callosum abnormalities using 3D ultrasound is insufficient. This is a reason why 3D ultrasound is not clinically applied in the routine screening methods of the brain [10]. In this study, only 31.5% of the structures on the median sagittal view were clearly identified, which was inconsistent with previous articles. The main reasons are as follows: (1) The previous reports of 3D ultrasound have mostly focused on the normal craniocerebral imaging of the corpus callosum [24], and this has been reported in the abnormal corpus callosum [27,28]. This study included 34 (16.7%) cases of corpus callosum abnormalities, and the lateral cerebral gyrus was arranged radially in CACC cases, similar to previous reports. However, 3D ultrasound is difficult to identify the gyrus structure; (2) As the "sentinel" of abnormal corpus callosum, cavum septi pellucidi plays an important role [29,30]. All the cases included in this study had an abnormal cavum septi pellucidi. Given the unclear boundary between the corpus callosum and the cavum septi pellucidi in the median sagittal view obtained from the 3D reconstruction, the reconstructed corpus callosum may actually be an overlap of the cingulate gyrus, cingulate sulcus, cerebrospinal fluid and the pericallosal artery [10].

Fetal brain MRI has the advantages of no ionizing radiation, multi-directional imaging, and high soft tissue resolution, and can directly display the development of the fetal ventricular system, brain tissue, and corpus callosum [31,32]. With the clinical application of rapid sequence, the fetal MRI image quality was significantly improved. Though there is a direct correlation between corpus callosum anomalies and the early-onset epilepsy of Aicardi Syndrome. However, corpus callosum anomalies cannot be the only factor responsible for the clinical outcome. Most of the aicardi patients with ACC had severe polymicrogyria and a higher number of heterotopic nodules [8]. Sotiriadis and Makrydimas [33] recognized that MRI could detect not only the classical association (such as Dandy Walker lineage and midline abnormalities), but also the cortical abnormalities, which can significantly alter the prognosis. In this study, MRI also diagnosed a case of penetrating brain malformation missed by ultrasound. In the classification of corpus callosal abnormalities, fetal MRI can effectively detect callosal abnormalities and can verify the presence or absence of ultrasoundidentified corpus callosum abnormalities satisfactorily and add value to improve clinical decision-making [11]. The International Association for Maternity Ultrasound (ISUOG) in 2021 (Part 2) again emphasized that MRI should be performed as a complementary method to specific neuro-ultrasonography [25].

In this study, the main reasons for the low consistency between ultrasound and magnetic resonance for HpCC are as follows: (1) It is difficult for ultrasound to identify the absence of the splenium of the corpus callosum and a short corpus callosum; (2) Based on ultrasound imaging principles and angle of incidence of sound beam, the ultrasound display of the rastrum of the corpus callosum is difficult. So it is not sensitive to the absence of the rastrum of the corpus callosum.

5. Conclusions

Prenatal ultrasound can accurately classify CACC and PACC, among which the diagnosis of ultrasound CACC is highly consistent with magnetic resonance. Magnetic resonance imaging can provide not only accurate classification but also other important prognostic information including tuberous sclerosis and cortical dysplasia when abnormalities of the corpus callosum are suspected by ultrasound. However, prospective studies are needed in order to explore new methods to further improve the consistency of ultrasound and magnetic resonance imaging in classifying abnormalities of the corpus callosum, as well as new ideas, to find more signs related to disease prognosis such as morphological study of sulcal gyrus.

Availability of Data and Materials

The data that support the findings of this study are available on request from the corresponding author.

Author Contributions

HP, XC, and JLZ designed the research study, HP, XJZ and XC performed the research, YS and CLC analyzed the data. All authors contributed to editorial changes in the manuscript. All authors read and approved the fi-

nal manuscript. All authors have participated sufficiently in the work and agreed to be accountable for all aspects of the work.

Ethics Approval and Consent to Participate

The retrospective study was approved by the Research Ethics Committee of Wenjiang District Maternal and Child Health Hospital, Sichuan Academy of Medical Sciences and written informed consent was obtained from all subjects (WJFY2022LSLY-032).

Acknowledgment

Not applicable.

Funding

This work was supported by Project of Chengdu Municipal Health Commission (No.2022384); Project of Chengdu Municipal Health Commission (No.2023365).

Conflict of Interest

The authors declare no conflict of interest.

References

[1] Rüland AM, Berg C, Gembruch U, Geipel A. Prenatal Diagnosis of Anomalies of the Corpus Callosum over a 13-Year Period. Ultraschall in Der Medizin. 2016; 37: 598–603. https://doi.org/10.1055/s-0034-1399699.

[2] Zeng Q, Wen H, Yuan Y, Ding Y, Liao Y, Luo D, *et al*. A novel technique to assess fetal corpus callosum by two-dimensional axial plane. European Radiology. 2020; 30: 5871–5880. https://doi.org/10.1007/s00330-020-06981-9.

[3] Edwards TJ, Sherr EH, Barkovich AJ, Richards LJ. Clinical, genetic and imaging findings identify new causes for corpus callosum development syndromes. Brain. 2014; 137: 1579–1613. https://doi.org/10.1093/brain/awt358.

[4] Horgos B, Mecea M, Boer A, Szabo B, Buruiana A, Stamatian F, *et al*. White Matter Dissection of the Fetal Brain. Frontiers in Neuroanatomy. 2020; 14: 584266. https://doi.org/10.3389/fnana.2020.584266.

[5] ENSO Working Group. Role of prenatal magnetic resonance imaging in fetuses with isolated mild or moderate ventriculomegaly in the era of neurosonography: international multicenter study. Ultrasound in Obstetrics & Gynecology. 2020; 56: 340–347. https://doi.org/10.1002/uog.21974.

[6] Di Mascio D, Sileo FG, Khalil A, Rizzo G, Persico N, Brunelli R, *et al*. Role of magnetic resonance imaging in fetuses with mild or moderate ventriculomegaly in the era of fetal neurosonography: systematic review and meta-analysis. Ultrasound in Obstetrics & Gynecology. 2019; 54: 164–171. https://doi.org/10.1002/uog.20197.

[7] Meidan R, Bar-Yosef O, Ashkenazi I, Yahal O, Berkenstadt M, Hoffman C, *et al*. Neurodevelopmental outcome following prenatal diagnosis of a short corpus callosum. Prenatal Diagnosis. 2019; 39: 477–483. https://doi.org/10.1002/pd.5460.

[8] Masnada S, Pichiecchio A, Formica M, Arrigoni F, Borrelli P, Accorsi P, *et al*. Basal Ganglia Dysmorphism in Patients With Aicardi Syndrome. Neurology. 2021; 96: e1319–e1333. https://doi.org/10.1212/WNL.0000000000011237.

[9] Marathu KK, Vahedifard F, Kocak M, Liu X, Adepoju JO, Bowker RM, *et al*. Fetal MRI Analysis of Corpus Callosal Abnormalities: Classification, and Associated Anomalies. Diagnostics. 2024; 14: 430. https://doi.org/10.3390/diagnostics14040430.

[10] Malinger G, Lerman-Sagie T, Viñals F. Three-dimensional sagittal reconstruction of the corpus callosum: fact or artifact? Ultrasound in Obstetrics & Gynecology. 2006; 28: 742–743. https://doi.org/10.1002/uog.3823.

[11] Manevich-Mazor M, Weissmann-Brenner A, Bar Yosef O, Hoffmann C, Mazor RD, Mosheva M, *et al*. Added Value of Fetal MRI in the Evaluation of Fetal Anomalies of the Corpus Callosum: A Retrospective Analysis of 78 Cases. Ultraschall in Der Medizin. 2018; 39: 513–525. https://doi.org/10.1055/s-0043-113820.

[12] Li S, Deng X. Guidelines for Ultrasound Examination (2012). Chinese Journal of Medical Ultrasound (Electronic Edition). 2012; 9: 574–580. http://doi.org/10.3877/cma.j.issn.1672-6448.2012.07.002. (In Chinese)

[13] Falco P, Gabrielli S, Visentin A, Perolo A, Pilu G, Bovicelli L. Transabdominal sonography of the cavum septum pellucidum in normal fetuses in the second and third trimesters of pregnancy. Ultrasound in Obstetrics & Gynecology. 2000; 16: 549–553. https://doi.org/10.1046/j.1469-0705.2000.00244.x.

[14] Karl K, Esser T, Heling KS, Chaoui R. Cavum septi pellucidi (CSP) ratio: a marker for partial agenesis of the fetal corpus callosum. Ultrasound in Obstetrics & Gynecology. 2017; 50: 336–341. https://doi.org/10.1002/uog.17409.

[15] Malinger G, Zakut H. The corpus callosum: normal fetal development as shown by transvaginal sonography. AJR American journal of roentgenology. 1993; 161: 1041–1043. https://doi.org/10.2214/ajr.161.5.8273605.

[16] Grogono JL. Children with agenesis of the corpus callosum. Developmental Medicine and Child Neurology. 1968; 10: 613–616. https://doi.org/10.1111/j.1469-8749.1968.tb02944.x.

[17] Jeret JS, Serur D, Wisniewski KE, Lubin RA. Clinicopathological findings associated with agenesis of the corpus callosum. Brain & Development. 1987; 9: 255–264. https://doi.org/10.1016/s0387-7604(87)80042-6.

[18] Knezović V, Kasprian G, Štajduhar A, Schwartz E, Weber M, Gruber GM, *et al*. Underdevelopment of the Human Hippocampus in Callosal Agenesis: An In Vivo Fetal MRI Study. AJNR. American Journal of Neuroradiology. 2019; 40: 576–581. https://doi.org/10.3174/ajnr.A5986.

[19] Innocenti GM, Ansermet F, Parnas J. Schizophrenia, neurodevelopment and corpus callosum. Molecular Psychiatry. 2003; 8: 261–274. https://doi.org/10.1038/sj.mp.4001205.

[20] D'Antonio F, Pagani G, Familiari A, Khalil A, Sagies TL, Malinger G, *et al*. Outcomes Associated With Isolated Agenesis of the Corpus Callosum: A Meta-analysis. Pediatrics. 2016; 138: e20160445. https://doi.org/10.1542/peds.2016-0445.

[21] He M, Du L, Xie H, Lei T, Zheng Q, Wu L. The ratio of cavum septi pellucidi width to anteroposterior cerebellar diameter: A novel index as a diagnostic adjunct for prenatal diagnosis of trisomy 18. The Journal of Obstetrics and Gynaecology Research. 2019; 45: 1245–1250. https://doi.org/10.1111/jog.13960.

[22] Shen O, Gelot AB, Moutard ML, Jouannic JM, Sela HY, Garel C. Abnormal shape of the cavum septi pellucidi: an indirect sign of partial agenesis of the corpus callosum. Ultrasound in Obstetrics & Gynecology. 2015; 46: 595–599. https://doi.org/10.1002/uog.14776.

[23] Choudhri AF, Cohen HL, Siddiqui A, Pande V, Blitz AM. Twenty-Five Diagnoses on Midline Images of the Brain: From Fetus to Child to Adult. Radiographics: a Review Publication of the Radiological Society of North America, Inc. 2018; 38: 218–235. https://doi.org/10.1148/rg.2018170019.

[24] Miguelote RF, Vides B, Santos RF, Palha JA, Matias A, Sousa N. The role of three-dimensional imaging reconstruction to measure the corpus callosum: comparison with direct mid-sagittal

views. Prenatal Diagnosis. 2011; 31: 875–880. https://doi.org/10.1002/pd.2794.

[25] Paladini D, Malinger G, Birnbaum R, Monteagudo A, Pilu G, Salomon LJ, *et al*. ISUOG Practice Guidelines (updated): sonographic examination of the fetal central nervous system. Part 2: performance of targeted neurosonography. Ultrasound in Obstetrics & Gynecology. 2021; 57: 661–671. https://doi.org/10.1002/uog.23616.

[26] Society for Maternal-Fetal Medicine (SMFM), Ward A, Monteagudo A. Absent Cavum Septi Pellucidi. American Journal of Obstetrics and Gynecology. 2020; 223: B23–B26. https://doi.org/10.1016/j.ajog.2020.08.180.

[27] Tarui T, Madan N, Farhat N, Kitano R, Ceren Tanritanir A, Graham G, *et al*. Disorganized Patterns of Sulcal Position in Fetal Brains with Agenesis of Corpus Callosum. Cerebral Cortex. 2018; 28: 3192–3203. https://doi.org/10.1093/cercor/bhx191.

[28] Vasung L, Yun HJ, Feldman HA, Grant PE, Im K. An Atypical Sulcal Pattern in Children with Disorders of the Corpus Callosum and Its Relation to Behavioral Outcomes. Cerebral Cortex. 2020; 30: 4790–4799. https://doi.org/10.1093/cercor/bhaa067.

[29] Borkowski-Tillman T, Garcia-Rodriguez R, Viñals F, Branco M, Kradjen-Haratz K, Ben-Sira L, *et al*. Agenesis of the septum pellucidum: Prenatal diagnosis and outcome. Prenatal Diagnosis. 2020; 40: 674–680. https://doi.org/10.1002/pd.5663.

[30] Society for Maternal-Fetal Medicine (SMFM), Rotmensch S, Monteagudo A. Agenesis of the Corpus Callosum. American Journal of Obstetrics and Gynecology. 2020; 223: B17–B22. https://doi.org/10.1016/j.ajog.2020.08.179.

[31] Glenn OA, Goldstein RB, Li KC, Young SJ, Norton ME, Busse RF, *et al*. Fetal magnetic resonance imaging in the evaluation of fetuses referred for sonographically suspected abnormalities of the corpus callosum. Journal of Ultrasound in Medicine. 2005; 24: 791–804. https://doi.org/10.7863/jum.2005.24.6.791.

[32] Cater SW, Boyd BK, Ghate SV. Abnormalities of the Fetal Central Nervous System: Prenatal US Diagnosis with Postnatal Correlation. Radiographics. 2020; 40: 1458–1472. https://doi.org/10.1148/rg.2020200034.

[33] Sotiriadis A, Makrydimas G. Neurodevelopment after prenatal diagnosis of isolated agenesis of the corpus callosum: an integrative review. American Journal of Obstetrics and Gynecology. 2012; 206: 337.e1–5. https://doi.org/10.1016/j.ajog.2011.12.024.